Proteomic and structural heart changes in obese rats are incompletely restored after weight loss

Arkadiusz Liśkiewicz (✉ adliskiewicz@gmail.com)

Medical University of Silesia, Faculty of Medical Sciences in Katowice, Katowice, Poland
https://orcid.org/0000-0002-4102-5373

Łukasz Marczak

Polska Akademia Nauk Instytut Chemii Bioorganicznej

Katarzyna Bogus

Slaski Uniwersytet Medyczny w Katowicach

Daniela Liśkiewicz

Akademia Wychowania Fizycznego imienia Jerzego Kukuczki w Katowicach

Marta Przybyła

Slaski Uniwersytet Medyczny w Katowicach

Joanna Lewin-Kowalik

Slaski Uniwersytet Medyczny w Katowicach

Original investigation

Abstract

Background As a systemic disorder, obesity strongly affects the cardiovascular system, inducing cardiac overgrowth, which increases the risk of heart failure and death. Moreover, obesity is potentially curable, leading to the restoration of the heart phenotype, but it is not clear if all of the after-effects are reversed after weight loss. of the heart phenotype, but it is not clear if all of the after-effects are reversed after weight loss. Here we describe the proteomic and morphologic phenotype of the heart in a rat model of developmental obesity with an evaluation of whether the observed effects are persistent in spite of weight loss.

Methods Developmental obesity with hyperlipidemia and insulin resistance was induced in young rats by exposure to a Western diet composed of human snacks. An histologic evaluation of the heart was performed to measure the size of the cardiomyocytes and amount of connective tissue discriminating the phenotype of obesity cardiomyopathy. The cardiac tissue and plasma were analyzed by global proteomic profiling. Based on these data, we targeted proteins for evaluation with the western blot. The histological and proteomic measurements were performed after weight loss to validate which features of obesity cardiomyopathy were persistent.

Results Obesity cardiomyopathy was determined as cardiac hypertrophy associated with fibrosis, oversized myocytes, and mTOR upregulation. A plethora of molecular changes were observed, suggesting an effect on the utilization of metabolic substrates in the hearts of obese animals. This was confirmed by increased levels of ACSL-1, a key enzyme for fatty acid degradation and decreased GLUT-1, a glucose transporter. Immunological processes and lipid metabolism were also affected in the cardiac tissue and plasma. Weight loss led to the normalization of the heart's size, but some after-effects of obesity such as connective tissue abundance and abnormal proteomic composition were still persistent.

Conclusion In addition to morphological consequences, obesity cardiomyopathy involves many proteomic changes. Obesity treatment and weight loss provides for a partial repair of the heart's architecture, but cardiac fibrosis and some proteomic alterations persist.

Background

According to International Statistical Classification of Diseases and Related Health Problems (10th revision), obesity is defined as a disorder characterized by an abnormally high, unhealthy amount of body fat and is listed as E66 subgroup of "endocrine, nutritional and metabolic diseases." This pandemic disease has many severe consequences including an increased risk of death, morbidity, and accelerated aging [1] due to the many systemic changes associated with obesity. The disease is widespread globally across all age groups [2, 3]. In the United States, 1 in 5 children are obese and the scale of the problem is well illustrated by reported cases of obesity among children. Obesity symptoms are potentially curable by losing weight due to reducing calorie intake and increasing energy expenditure. Other methods that are effective for weight loss include medication and surgery [4]. Reversing obesity is essential for lifespan

and healthspan because it affects all the systems of the human body, especially contributing to the development of cardiovascular diseases [5]. Obesity and the Western diet are leading causes of hypertension [6]. A pressure overload leads to pathological cardiac hypertrophy and overgrown myocytes enmeshed within an abundant network of the extracellular matrix (ECM) is the hallmark of obesity cardiomyopathy and left ventricle (LV) remodeling [7]. Although pressure overload is the predominant inductor of LV hypertrophy [8], the hypertrophied heart develops independently of hypertension during obesity [9], suggesting that other mechanisms may also contribute to the cardiac overgrowth. The hypertrophy of cardiomyocytes with cardiac fibrosis and remodeling associated with the Western diet and weight gain may be a consequence of the intensification of intracellular anabolic processes and sustantiation of a pro-inflammatory status [10, 11]. Normally cardiac fibroblasts make up about 70% of cardiac cells and support cardiomyocytes by producing ECM and by regulating the proliferation and migration of other cardiac cells [12]. Thus, fibroblasts play an important role in cardiac repair. However, in certain circumstances the excessive proliferation and differentiation of fibroblasts lead to the increased deposition of fibrotic content (fibrosis) and consequently to heart failure [13].

Weight reduction and weight loss maintenance is capable of reversing many of the alterations in cardiac performance and morphology associated with obesity [14] and is essential in avoiding heart failure related to obesity cardiomyopathy [15–17]. However, more detailed investigations are needed in order to identify the potential changes that are persistent after weight loss and to find treatment options.

This study uses animal models to demonstrate how developmental obesity affects the heart's proteome and morphology and identifies changes that are not reversed following weight normalization.

Materials And Methods

Dietary induced obesity

All animals were provided by the Animal House of the Department for Experimental Medicine, Medical University of Silesia, Katowice, Poland and were treated in accordance to Directive 2010/63/EU for animal experiments using the protocols approved and monitored by the Local Ethics Committee for Animal Experimentation in Katowice. Animals were housed 4–5 per cage in a climate-controlled room (22 ± 2 °C, relative humidity: 55 ± 10%) with a 12 h:12 h light/dark cycle starting at 07:00 a.m.

28-day-old Long Evans male rats were used in two independent experiments. In Exp.1, animals were fed ad libitum with standard chow (control to obese cohort, ContO) or the same chow supplemented with Western diet foods (Obese). These included cheese, dry sausage made of pork (kabanos), crackers, salty potato chips, candy bars (bounty, mars, prince-polo) and a 10% saccharose solution to drink. Additionally, all animals had unlimited access to drinking water. After 10 weeks the animals were euthanized by decapitation to collect blood and heart samples.

In Exp. 2, animals from the AWL group (After Weight Loss) were treated in the same manner as in Exp. 1 to develop obesity, but this was extended for 2 more weeks (12 weeks of weight gain). After this time the

rats were subjected only to standard rodent chow with an 80% calorie restriction (CR; the 100% of caloric needs was established empirically), which was reduced to 70% after two weeks until the end of the weight-loss-phase. During this period the control group from Exp. 2 (ContA) received the same isocaloric food to stop subtle weight gain in these control adult rats. The amount of food was established empirically for every cage and 20 g of standard chow/rat/day determined the criteria. After the period of weight reduction, the rats from AVL and ContA groups received an isocaloric amount of food for two weeks (stabilization phase) to equalize the calorie intake among control and experimental groups. Drinking water was provided ad libitum during all phases of Exp. 2.

Six hours prior to insulin tolerance and glucose loading tests the rats were fasted (tested animals from Exp.1 were fed by standard chow and water for 24 h before fasting), than insulin (1 U/kg in Exp.1; 0.75 U/kg in Exp.2; ActiRapid, Novo Nordisc) or glucose (2 g/kg) were injected in i.p. injections. Blood was collected from the tip of tail at the appropriate time intervals to measure glucose levels (CardioCheck Professional).

For the histological examination of the morphology of cardiomyocytes, 6 hearts per group collected during Exp. 1 and Exp. 2 were gently squeezed to remove excess blood, then weighed and immersed in a 10% formalin solution in PBS (pH = 7.2). For proteomic examination, fresh pieces of LV were collected from another animals (n = 5 per group in Exp. 1).

After decapitation ~ 2 mL of trunk blood was collected for serum and plasma samples. For the serum collection, the blood was allowed to clot by leaving it for 30 min on ice. The samples were then centrifuged (2,000 × g for 15 minutes, 4C), and the serum was pipetted and stored at − 80 °C. Serum cholesterol and triglyceride levels were measured in the sera using a Mindray BS-200 Chemistry Analyzer (Shenzhen Mindray Bio-Medical Electronics Co.).

For the plasma (used for proteomic profiling), 1 ml of blood was collected into 1.5 ml EDTA coated Eppendorf tubes containing 10 ul of 0.5 M EDTA and immediately centrifuged (1300 × g for 10 minutes, 4C). 99 ul of plasma was pipetted to fresh tubes containing 1 ul of a protease inhibitor cocktail (#P8340, Sigma Aldrich) [18].

Histological examination of the heart

The LV was dissected from formalin-fixed hearts. The tissues were dehydrated with graded concentrations of alcohol and embedded in paraffin. 5 μm paraffin slices from each tissue sample were stained with (1) Hematoxylin and Eosin (H&E) or (2) Masson's trichrome stain.

To calculate the cross-sectional area of the cardiomyocyte, the sections stained with H&E were photographed (with 40x objective) using a Nikon light microscope (Nikon ECLIPSE E600) with an Olympus Camera (Olympus DP 26). The individual cell surface area was measured by a blinded observer using cellSens Entry Imaging Software (Olympus). One hundred cell surface areas were counted per each group, and the average value was used for analysis.

Masson's stain was used to investigate LV morphology and perivascular/interstitial fibrotic changes. The sections were photographed (with 40x objective) 6 times each for the following: LV area without visible vessels (interstitial zone) and area with visible vessels (perivascular zone) [19]. The photos were subjected to deconvolution in the NIH Fiji program [20], than the areas of blue (connective tissue) or red (myocytes) channels were automatically counted. The data is expressed as the amount of connective tissue relative to the total area (connective tissue + myocytes) and expressed as a %.

Proteomic profiling

Protein extraction

The isolated brain tissues were lysed in a buffer with 1 M triethylammonium bicarbonate (TEAB) and 0.1% sodium dodecyl sulfate (SDS) and automatically homogenized using a Precellys 24 homogenizer (Bertin Technologies) in 0.5-mL tubes pre-filled with ceramic (zirconium oxide) beads (Bertin Technologies). Next, the material was subjected to a threefold cycle of freezing and thawing. Then, the tissue in the buffer was sonicated in a bath for three 1-minute cycles on ice and homogenized again using the Precellys 24 instrument. The protein concentration was measured using Pierce BCA protein assay kit (Thermo Fisher Scientific) in the isolated protein fraction according to the manufacturer's instructions.

In-solution digestion

Ten-microgram aliquots of the proteins were diluted with 15 µl of 50 mM NH4HCO3 and reduced with 5.6 mM DTT for 5 min at 95 °C. The samples were then alkylated with 5 mM iodoacetamide for 20 min in the dark at RT. The proteins were digested with 0.2 µg of sequencing-grade trypsin (Promega) overnight at 37 °C.

Liquid chromatography-tandem mass spectrometry (LC-MS/MS) analysis of the proteins

The analysis was performed with the use of the Dionex UltiMate 3000 RSLC nanoLC System connected to the Q Exactive Orbitrap mass spectrometer (Thermo Fisher Scientific). The peptides derived from the in-solution digestion were separated on a reverse phase Acclaim PepMap RSLC nanoViper C18 column (75 µm × 25 cm, 2 µm granulation) using an acetonitrile gradient (from 4 to 60%, in 0.1% formic acid) at 30 °C and a flow rate of 300 nL/min (for 230 min). The spectrometer was operated in data-dependent MS/MS mode with survey scans acquired at a resolution of 70,000 at m/z 200 in MS mode, and 17,500 at m/z 200 in MS2 mode. The spectra were recorded in the scanning range of 300−2000 m/z in the positive ion mode. Higher energy collisional dissociation (HCD) ion fragmentation was performed with normalized collision energies set to 27.

Data analysis of the proteins

Protein identification was performed using the Swiss-Prot rat database with a precision tolerance set to 10 ppm for peptide masses and 0.08 Da for fragment ion masses. All raw data obtained for each dataset

was imported into MaxQuant 1.5.3.30 version for protein identification and quantification. Protein was considered as positively identified if at least two peptides per protein were found by the Andromeda search engine, and a peptide score reached the significance threshold FDR = 0.01.

The obtained data was exported to Perseus ver. 1.5.3.2 software (part of the MaxQuant package). The numeric data was transformed to the logarithmic scale and each sample was annotated with its group affiliation. Next, the data was filtered based on valid values – proteins, which had valid values in 70% of samples in at least one group were kept in the table. A one-way analysis of variance (ANOVA) analysis was performed on the analyzed sample data with permutation-based FDR 0.05 used for truncation and the resulting list of differentiating proteins was normalized using a Z-score algorithm for the hierarchical clustering of data.

Gene ontology term analysis

Gene ontology (GO)-term enrichment analysis was performed with the DAVID functional annotation tool [21, 22]. The complete list of Rattus norvegicus proteins detected in mass spectrometry-based proteomics was used for the background and the GO term subcategories 'GOTERM_BP_DIRECT' 'GOTERM_CC_DIRECT' and 'GOTERM_MF_DIRECT' 'INTACT' were selected for analysis. An modified Bonferroni correction of p-value was applied to identify the statistically more represented function annotations

Immunoblotting

For immunoblotting, the samples were separated on 4–15% Stain-Free Gel (Bio-Rad) and transferred onto PVDF membranes. The membranes were blocked for 1 h at room temperature in Casein Blocking Buffer (Sigma-Aldrich) or 5% BCA, and incubated overnight at 4 °C (TBST + adequate blocking buffer) with primary antibodies produced in rabbits: anti-phospho AMPKα (Thr172) (Cell Signaling, #2535), anti-phospho mTOR (Thr2446 and Ser2448) (#15–105, MERK Millipore), anti-GLUT-4 (#PA1-1065, Invitrogen), anti-GLUT-1 (#ab652, Abcam), and anti-ACSL-1 (#PA5-17136, Invitrogen). After washing, the membranes were incubated with secondary donkey anti-rabbit IgG antibody (Abcam, ab205722). The immunoblots were visualized by means of Clarity Western ECL Blotting Substrates (Bio-Rad) and detected with the ChemiDoc™ Touch Imaging System (Bio-Rad). The targeted proteins were quantified with ImageLab Software 6.0.1 (Bio-Rad). The results were normalized to the total protein content in the gel (Stain-free technology, Bio-Rad).

Statistical analysis

Statistical analysis was performed using GraphPad Prism 8.01 software (GraphPad Software Inc.). Depending on the data distribution (as evaluated by the Shapiro-Wilk normality test), either the Student's T-test or U-Mann-Whitney test were used for the estimation of significant differences between the two subject groups. In the case of repeating measurements, two-way ANOVA with Sidak's multiple comparison test was applied. In all tests, significance was considered when $p < 0.05$.

Results

The obesity phenotype is associated with heart hypertrophy

In order to evaluate the influence of developmental obesity on the heart proteomic profile, the rats were fed with a Western diet starting from the 28th day of life for 10 weeks. Starting with the 3rd week of feeding, these rats gained weight more excessively than control individuals (Fig. 1A). The obesity phenotype resulted in decreased response to insulin measured by ITT (Fig. 1B). An analysis of sera revealed higher triglycerides (p = 0.0007) and LDL (p = 0.03) concentrations in obese rats (Fig. 1C). These rats also had increased total-cholesterol-to-HDL ratio (p = 0.0006, Fig. 1C), which is recognized as a strong cardiovascular risk marker [23]. Ten weeks after introduction of dietary-induced obesity protocol, the authors collected the hearts from animals to perform morphometric and proteomic analyses. The hearts of obese rats were about 35% heavier than in control individuals (p < 0.0001; Fig. 2A). The histological examination of H&E-stained LV sections revealed that the cardiomyocytes in obese rats had increased an area as compared to control individuals (p = 0.0015) (Fig. 2B). The microscopic evaluation of Masson-Trichrome stained slides revealed a higher amount of connective tissue immersed between the myocytes (Fig. 2C) or localized around the vessels (Fig. 2D). The enhanced phosphorylation of mTOR on Ser2448 was observed in the LV of obese rats (p = 0.016) (Fig. 2E), suggesting the up-regulation of this anabolic pathway. On the other hand, the phosphorylation of mTOR on Thr2446 did not differ among groups (Fig. 2F). This mTOR region is phosphorylated during AMPK activation resulting in mTOR pathway inhibition [24]. In line with this, the authors did not observe significant changes in AMPK signaling (Fig. 2G).

The proteomic status of the cardiac cells exhibited a stronger shift towards the utilization of fatty acids in obese animals

By means of global proteomic profiling the pool of 86 proteins significantly changed in the LV of obese rats was identified (Fig. 3, heatmap), revealing that this phenotype strongly determined the composition of the cardiac tissue (Fig. 4A). Based on the GO database (GO: CC), the analysis of proteomic data revealed that the localization of significantly different proteins was mostly extracellular (extracellular exosomes, ~ 63%, p < 0.001), but also mitochondrial (36%, p < 0.001) and cytoplasmic (~ 27%, p < 0.001) (see Supplemental Data for more details). The data showed that two biological processes (GO: BP) are changed in the hearts of obese rats: the directed movement of phospholipids out of a cell or organelle (phospholipid efflux, p = 0.024, Fig. 4B) and the chemical reactions and pathways involving ATP (ATP metabolic process, p = 0.043, Fig. 4C). ~47% of the protein pool interacted (INTACT database, Fisher correction) with two proteins: solute carrier family 2, facilitated glucose transporter member 4 (GLUT-4, 27 proteins interacted significantly, p < 0.001) and acyl-CoA synthetase long-chain family member 1 (ACSL-1; 4 proteins interacted significantly, p = 0.0035). When the protein pool was analyzed separately depending

on whether the proteins were overexpressed or downregulated in the LV of obese rats, the subset of 40 elevated cardiac proteins confirmed the significant interaction with ACSL-1, whereas a subgroup of the remaining proteins (decreased expression in obese animals) interacted with GLUT-4. Thus the authors decided to perform the western blot to assess the expression of these two molecules. The level of ACSL-1 was significantly increased in the LV of obese rats (Fig. 4D, $p = 0.045$). In spite of the fact that cardiac GLUT-4 is downregulated [25] during insulin resistance, the authors did not clearly demonstrate its decreased content in the heart of obese rats (Fig. 4E). Rather than by transcriptional mechanisms, the regulation of GLUT-4 depends on its recruitment to the sarcolemma in response to glucose delivery and prolonged hyperinsulinemia leads to the internalization and inactivation of this glucose carrier. In addition to GLUT-4, the most abundant glucose transporter in the heart is solute carrier family 2, facilitated glucose transporter member 1 (GLUT-1) [26], thus it was decided to measure its expression. The authors have observed the decreased content of GLUT-1 (Fig. 4F, $p = 0.025$), which is an insulin-independent glucose transporter mainly responsible for the basal needs of the muscle cells [27]. As it was shown that Acsl1 knockout mice upregulate GLUT-1 expression in skeletal [28] and cardiac [29] muscles depending on glucose metabolism, it is possible that that ACSL-1 and GLUT-1 expression depend on each other.

The biological processes involved in the regulation of the immune system and triglycerides homeostasis are changed in the plasma of obese rats

Next, the authors performed global proteomic measurement in the plasma of the rats, identifying 41 molecules which differentiate between groups (Fig. 5, heatmap). Based on the results of DAVID analysis, eight biological processes (GO: BP) were changed in the plasma of obese rats, including i.e. the process that decreases the frequency, rate, or extent of endopeptidase activity (negative regulation of endopeptidase activity, $p < 0.001$), immunological responses (complement activation, $p < 0.001$; acute-phase response, $p < 0.001$; inflammatory response, $p < 0.05$), and processes that change the state or activity of a cell as a consequence of triglyceride stimulus (response to triglyceride, $p < 0.05$). Figure 5 presents the protein involved in these biological processes except for the negative regulation of endopeptidase activity (Supplemental Data). Due to the fact that various molecules participate in different immunologic processes, the proteins of acute and inflammatory responses have been combined (Fig. 6). Changes of four exosomal molecules detected in the LV were also significant in the plasma of obese rats (Supplemental Data). Alpha-1-inhibitor III, apolipoprotein A4 (APOA4), and apolipoprotein C3 (APOC3) were increased in both tissues. Transthyretin (TTR; thyroid hormone-binding protein) was elevated in the heart but decreased in the plasma of obese rats.

CR-induced weight loss partially restored the heart's architecture, leaving fibrotic debris

Another cohort of young animals was subjected to a Western diet for 12 weeks to gain weight and then to a 6-week-long CR protocol to reduce weight (AWL group; Fig. 7A). The group was accompanied by control animals (ContA group) which were maintained exclusively on a standard diet. This was followed by two subsequent weeks of isocaloric feeding to normalize the systemic parameters in both AWL and ContA groups. Obesity-induced insulin insensitivity and applied CR could reverse it, even resulting in higher insulin sensitivity [30], but there were no significant differences in the response to insulin (Fig. 7B) or glucose (Fig. 7C) in AWL rats. Hyperlipidemia was also reversed after weight loss (refer to the Supplemental Data). The authors observed that the weight of the collected hearts did not differ among AWL and control animals (Fig. 6D) and the histologic examination did not reveal any differences in the size of the cardiomyocytes among groups (Fig. 6E). However, the amount of interstitial (Fig. 7F) and perivascular (Fig. 7G) connective tissue was elevated in the LV of AWL rats, suggesting persistent cardiac fibrosis in individuals which were obese in the past.

The identification of cardiac and systemic proteomic hallmarks of obesity persist after weight loss

Proteomic data revealed that the concentration of 13 identified proteins and 1 unknown molecule were still altered in the hearts of the rats after weight loss (Table 1). Two proteins – adenylate kinase 1 and complement C3 – were changed in the hearts of both obese and AWL rats. Ak1 was decreased in both obese and AWL groups. However, complement C3 was elevated in the hearts of obese rats but decreased in AWL individuals (Supplemental Data). The analysis of the plasma revealed that 15 identified proteins (and one unknown) varied in the plasma of AWL and control rats (Table 2), but none of these molecules were noted to be changed in the plasma of obese rats. These proteins are mostly involved in the regulation of endopeptidase activity (8 proteins, $p < 0.001$), complement activation (4 proteins, $p < 0.001$), and chemical reactions and pathways involving hyaluronanhyaluronian (3 proteins, $p < 0.01$). The extracellular protein TTR, responsible for the transport of thyroxin and retinol binding protein complex to the various parts of the body, was decreased in the plasma of AWL rats ($p = 0.004$). In the plasma, TTR binds to adipokine known as retinol-binding protein 4 (RBP4), which prevents glomerular filtration and the subsequent catabolism of RBP4 in the kidney. However, despite TTR depletion RBP4 levels were elevated ($p = 0.048$). TTR may be used as a biomarker of stress disorders [31], oxidative stress [32], lean body mass, and catabolic states [33]. RBP4 was shown as a marker of insulin resistance [34], but these results are inconclusive [35]. Several human and animal studies have investigated the influence of high circulating RBP4 levels in the pathogenesis of insulin resistance associated with type 2 diabetes and obesity [35]. The current data suggest that the systemic balance between TTR and RBP4 may be disturbed after weight loss, but this phenomenon warrants further evaluation.

Table 1

Proteins significantly changed (Students's T test) in the cardiac muscle of rats from AWL (After Weight Loss) group as compared to control individuals.

Cellular Compartment	UNIPROT	Name: protein (gene)	AWL vs. control	Function/biological process
mitochondrion	B5DEF6	acyl-CoA dehydrogenase family, member 10 (Acad10)	↑	fatty acid beta-oxidation
extracellular exosome	A0A0G2K7Q6	adenylate kinase 1(Ak1)	↓	catalyzes the reversible transfer of the terminal phosphate group between ATP and AMP
mitochondrion	Q6P784	branched chain amino acid transaminase 2 (Bcat2)	↓	catalyzes the first reaction in the catabolism of the essential branched chain amino acids leucine, isoleucine, and valine
extracellular exosome/extracellular matrix	P45592	cofilin 1(Cfl1)	↓	controls reversibly actin polymerization and depolymerization in a pH-sensitive manner
extracellular exosome	P01026	complement C3(C3)	↓	plays a central role in the activation of complement system (a part of the immune system)
mitochondrion	P12007	isovaleryl-CoA dehydrogenase (Ivd)	↓	mitochondrial matrix enzyme that catalyzes the third step in leucine catabolism
extracellular exosome/extracellular matrix	P51886	Lumican (Lum)	↑	collagen fibril organization
mitochondrion	Q5XIG4	OCIA domain containing 1 (Ociad1)	↑	regulation of stem cell differentiation
cytosol	Q5M819	phosphoserine phosphatase (Psph)	↑	catalyzes the last step in the biosynthesis of serine from carbohydrates

Cellular Compartment	UNIPROT	Name: protein (gene)	AWL vs. control	Function/biological process
mitochondrion	Q75Q41	translocase of outer mitochondrial membrane 22 (Tomm22)	↑	interacts with TOMM20 and TOMM40, and forms a complex with several other proteins to import cytosolic preproteins into the mitochondrion
mitochondrion/extracellular exosome	Q75Q39	translocase of outer mitochondrial membrane 70 (Tomm70)	↑	receptor that accelerates the import of all mitochondrial precursor proteins
cytosol/cytoskeleton	Q6P9T8	tubulin, beta 4B class IVb (Tubb4b)	↓	major constituent of microtubules
extracellular exosome	Q00981	ubiquitin C-terminal hydrolase L1 (Uchl1)	↓	ubiquitin-protein hydrolase involved both in the processing of ubiquitin precursors and of ubiquitinated proteins
N/A	Q7TMZ9	unknown protein	↑	N/A

Table 2

Proteins significantly changed (Student's T test) in the plasma of rats from AWL (After Weight Loss) group as compared to control individuals. All of the identified proteins are extracellular and secreted by exosomes.

UNIPROT	Name: protein (gene)	AWL vs control	Function/biological process
M0RBF1	complement C3 (C3)	↓	plays a central role in the activation of the complement system
A0A096P6L9	complement C5 (C5)	↓	derived from proteolytic degradation of complement C5, C5 anaphylatoxin is a mediator of local inflammatory process.
Q5BKC4	complement C9 (C9)	↓	component of the terminal complement complex C5b-9, which induces cleavage and activation of caspase 3 and mediates induction of apoptosis
A0A5C5	complement component 4 binding protein, beta (C4bpb)	↓	controls the classical pathway of complement activation
Q6MG74	complement factor B (Cfb)	↓	complement activation
P20059	Hemopexin (Hpx)	↓	binds heme and transports it to the liver for breakdown and iron recovery, after which the free hemopexin returns to the circulation
D3ZBS2	inter-alpha trypsin inhibitor, heavy chain 3 (Itih3)	↓	a carrier of hyaluronan in serum
D3ZFH5	inter-alpha-trypsin inhibitor heavy chain 2 (Itih2)	↓	a carrier of hyaluronan in serum
Q5EBC0	inter-alpha-trypsin inhibitor heavy chain family, member 4 (Itih4)	↓	type II acute-phase protein (APP) involved in inflammatory responses to trauma
A0A1K0FUB2	myoglobin (Mb)	↑	serves as a reserve supply of oxygen and facilitates the movement of oxygen within muscles
B2RZC1	retinol binding protein 4 (Rbp4)	↑	delivers retinol from the liver stores to the peripheral tissues
P31211	corticosteroid-binding globulin (Serpina6)	↓	major transport protein for glucocorticoids and progestins in the blood of almost all vertebrate species

UNIPROT	Name: protein (gene)	AWL vs control	Function/biological process
Q5M7T5	antithrombin (Serpinc1)	↓	inhibits thrombin as well as other activated serine proteases of the coagulation system, and it regulates the blood coagulation cascade
A0A0G2K8K3	serpin family D member 1 (Serpind1)	↓	thrombin inhibitor activated by the glycosaminoglycans, heparin or dermatan sulfate
P02767	transthyretin (Ttr)	↓	thyroid hormone-binding protein. Probably transports thyroxine from the bloodstream to the brain
E9PSU8	unknown protein	↓	-

Discussion

Here, we discriminate the proteomic and morphological consequences of obesity in the hearts of rats accompanied by an evaluation of whether the changes are reversed by CR-induced weight loss. The presented data shows that the altered proteomic status and excessive amount of connective tissue can be found in the LV after returning to a normal body weight. This conclusion has not been recognized thus far.

Morphological and molecular characteristics of the heart in obesity

The phenotype of obesity cardiomyopathy includes heart hypertrophy with an increased amount of interstitial and perivascular connective tissue [36]. The upregulation of the mTOR pathway is predominantly involved in this cardiac remodeling [37] as a consequence of overfeeding and insulin resistance [38]. Therefore, we observed enlarged cardiomyocytes and increased mTOR phosphorylation suggesting the upregulation of this anabolic process in the cardiac cells of obese rats. We assumed that decreased AMPK signaling, as a possible consequence of overfeeding, may be partially involved in the mTOR control, but AMPK phosphorylation and its targeted site on mTOR (Thr2446, leading to its inhibition when phosphorylated [24]) seem to be unaffected, rejecting the assumption above. Further, the observed cardiomyopathy was reflected in a plethora of molecular changes. The proteomic machinery responsible for the transport of triglycerides was boosted in obese animals both in the plasma and the heart muscle. In order to metabolize long-chain fatty acids, they must first be converted to acyl-CoA by ACSL proteins [39]. Among the five mammalian ACSL isoforms, ACSL-1 predominates in the cardiac tissue [40]. The hearts of obese rats expressed more ACSL-1 but had reduced amounts of GLUT-1. These findings suggest that in obesity cardiomyopathy, glucose uptake may be decreased in favor of lipid metabolism. Whereas energetic metabolism in the normal heart depends primarily on ß-oxidation and

less on glucose utilization, in the diabetic heart ATP production becomes almost completely reliant on fatty acids oxidation [41, 42], causing the inability to switch between energetic substrates in case of trauma. The inability of efficient ATP generation from glucose under specific pathological conditions contributes to heart failure [43].

The results of some previous studies, where non-targeted proteomic methods were applied for the screening of cardiac tissue in animal model of dietary induced obesity, are mostly consistent with our observations. A map of the cardiac proteome in obese rats showed that the proteins involved in regulation of metabolism were predominantly changed [44]. The proteomic machinery responsible for fatty acids uptake and oxidation was upregulated in obese animals without hypertrophied hearts [44]. Thus the role of boosted fatty acids turnover in the cardiac remodeling is doubtful. In the mice with dietary induced obesity the expression of the proteins involved in mitochondrial metabolism was affected, resulting in production of reactive oxygen species [45–47]. This is probably a consequence of the excessed delivery of fats which are intensively metabolized in cardiomyocytes [48]. Although substantial protein expression changes the in obesity the cardiac proteome may be also affected in a different way, by modifying pattern of acetylation [49].

Most of the LV proteins affected by obesity originated from exosomal vesicles, raising the importance of these molecules in the pathomechanisms of obesity cardiomyopathy. Exosomes are the smallest extracellular vesicles (diameter, 30–100 nm) next to microvesicles (100–1000 nm) and apoptotic bodies (500–4000 nm). Six main types of cardiac cells, i.e., fibroblasts, cardiomyocytes, endothelial cells, cardiac progenitor cells, adipocytes, and cardiac telocytes, release exosomes carrying different cargo and enforcing various responses [50]. All of these cell types use extracellular molecules to communicate with each other and any alteration either in the composition of the exosomal cargo or its machinery can affect cardiac homeostasis, leading to disease [13]. Cardiac exosomes are oversecreted as a consequence of stressing factors such as angiotensin II production, hypoxia, inflammation, or injury [51]. Recent literature has shown that exosomes may modify cardiac repair and the fate of fibrosis via the modulation of fibroblast function and likely contribute to obesity cardiomyopathy in which microRNAs seem to play a crucial role [13]. For example, it was proposed that cardiac fibrosis in diabetic cardiomyopathy may be a consequence of the increased exosomal secretion of microRNA-320, a negative regulator of Heat shock protein 20 expression. Moreover, the overexpression of heat shock protein 20 remarkably attenuated diabetes-induced cardiac dysfunction and adverse remodeling [52]. Here we have observed an obesity-related decrease in cardiac heat shock 70 kDa protein, which normally protects cells against various types of stress [53] and is downregulated in obesity [54]. Its role can be considered in targeting obesity cardiomyopathy.

The cardiac outcomes of obesity reflect systematic disturbances

The proteomic composition of the plasma in obese rats strongly supports the notion that the systemic consequences of obesity and the Western diet are reflected in the cardiac muscle. Increased

angiotensinogen levels led to the suspicion that obese rats developed hypertension with the involvement of the renin–angiotensin system [55], and this could contribute to the overgrowth of cardiomyocytes [56]. Apolipoproteins are master regulators of plasma lipoprotein particles (HDL, LDL and chylomicrons), the carriers of fats and cholesterol in the body. APOA4 and APOC3 apolipoproteins were increased in the plasma of obese rats. APOC3 overproduction is especially noteworthy because of driving the risk of cardiovascular disturbances [57] and can be postulated as a therapeutic target to reduce the disease's development [58]. Moreover, four apolipoproteins were elevated in the heart (apolipoprotein A1, APOA4, APOC3, and apolipoprotein E), suggesting the high vulnerability of cardiac tissue towards the lipidomic changes accompanying dietary-induced obesity.

Apoa4 is expressed almost exclusively in the intestine and released into the blood in chylomicrons transporting dietary-derived fatty acids. Apolipoprotein E is more widely expressed, but predominantly by the adrenal gland, brain, and liver. These proteins were elevated in the heart muscle but also in plasma of obese rats possibly as a consequence of its higher concentration in the blood. Apolipoprotein A1 and APOC3 levels were elevated in the heart, but they are expressed in the liver and intestine and apparently their cardiac accumulation accompanied the influx of lipids and cholesterol to the heart [59–61]. Decreased levels of gelsoline indicates pathological conditions as this protein normally occurs in high amounts and is extensively degraded when binding to filamentous actin (released upon cell death or rupture) occurs [62]. This protein mitigates the detrimental effects of systemic inflammation [63], thus gelsoline downregulation could potentiate a greater impact of obesity-related inflammation on the system. Protein clustering revealed that obese animals developed contradictory inflammatory status. On the one hand, chronic inflammation elevated pro-inflammatory molecules such as fibronectin [64] and haptoglobin [65] in obese animals. Inconsistently, α1-inhibitor-3 [66] and kininogens [67] known as pro-inflammatory factors were decreased. This was associated with the downregulation of anti-inflammatory α1-antitrypsin [68] and transferrin, which is negatively regulated during the acute phase [69]. On the other hand, the defense response could be diminished, which was recognized as the decreased expression of the complement system proteins being a part of the immune system launched during a pathogen attack [70].

Weight loss reverse cardiac overgrowth but not fibrotic deposition

Obesity evokes cardiac remodeling, which seems to be rescued after weight loss [17, 36]. However, a significant finding of our study was that after weight loss the heart is still abundantly composed of connective tissue. We suspect that this could be a residue of obesity as well as a consequence of CR applied for weight reduction. Whereas intracellular compartments in the cardiomyocytes are degraded via autophagy, allowing for tissue rearrangement, the redundant ECM is proteolyzed and then digested by the phagocytic cells of the complement immune system [71]. The proteins of the complement cascade were downregulated in the heart collected after weight loss, suggesting that inflammatory response and the recruitment of phagocytic cells is rather repressed than mobilized. Such a cardiac immunosuppression could diminish the complete restoration of tissue during weight loss. Due to the novelty of this thesis,

more research is required to support its authenticity. However, there may be an additional reason for the observed elevation of the heart's connective tissue after weight reduction. CR impacts cardiac morphology in an age-dependent manner by stimulating the fibrotic deposition in young-adult mice (age-matched to our rats), but not in older animals, emphasizing the possible cardiac residue of CR [72].

The different proteomic composition of the LV in AWL rats may be a consequence of cardiac fibrosis and ECM excess, which is illustrated by the lower amount of cardiac tubulin as this protein is abundantly expressed in the myocytes but scarce in ECM [73]. Conversely, the pool of lumican was elevated in the hearts of AWL rats. Lumican is a proteoglycan which binds collagens, the main components of cardiac ECM [74], therefore its level correlates with the deposition of fibrocytes representing tissue fibrosis. Lumican expression is increased in hepatic [75], pulmonary [76], and cardiac [74] fibrosis. On the one hand, experimental and clinical findings revealed that the overexpression of lumican in cardiac fibroblasts is evoked during heart failure [74]. This protein regulates cardiac remodeling following LV pressure overload [77] and has been shown to have a role in ECM remodeling and fibrosis in different cardiovascular diseases [78–80]. On the other hand, lumican is required for cardiac remodeling by ensuring the structural integrity of connective tissue and survival following pressure overload [77]. We propose that lumican may play a role in obesity-related cardiac remodeling and we observed that its levels are elevated after weight loss, carrying the possible risk of fibrosis-related disturbances.

Limitations of the study and transferal of the results

The rat model of dietary-induced obesity was introduced to reflect developmental obesity. Thus the animals were young (28 days old) at the time the Western diet was introduced, reflecting ~ 8 months of human age [81] when infants begin receiving solid food [82]. The overconsumption of protein and sugars especially induce developmental obesity [83], and the global intake of the latter range from 1.9–13.4% in humans before 2 years of age [84] underlies the high dietary risk factors for the development of obesity in infants. Comprehensive proteomic evaluation was performed in the plasma and cardiac tissue of obese and CR-cured rats. In the second group, the tissue material was collected after two weeks of isocaloric intake, where AWL rats and control companions received the same amount of calories, allowing for weight maintenance without significant weight gain or reduction. This approach seemed to be the most reasonable and made it somewhat possible to eliminate the systemic effects of CR [85]. The animals could not be fed by standard chow in an ad libitum manner because from our experience, AWL rats regain weight more extensively than control individuals. Thus, during the "stabilization state" both groups received ~ 100% of calorie needs, which was set empirically. We did not find any justification to compare the effects observed in obese animals with AWL rats and adequate controls (by comparing the four groups in parallel), especially considering the different age of the animals. In such a comparison we would not estimate the impact of body weight only, but also the age factor, thereby falsifying the conclusion.

The prevalence of obesity actually increased with hordes of young people predisposed to weight-loss therapies. If adequate approaches will be applied to reduce body weight, these patients could be rescued from obesity within a few years [86]. The restoration of a lean phenotype masks the obesity experience,

possibly shaping future diagnosis in adulthood or the elderly. However, the persistent effects of obesity are not well explored. What if by disregarding the bygone obesity the true reason for the current disability will be obscured? We suggest that clinicians should consider the possibility of the persisting cardiac consequences of obesity in lean patients during diagnosis.

Conclusion

Global proteomic profiling with morphological evaluation was performed in the hearts of obese rats and after weight loss. We conclude that obesity cardiomyopathy is highly complex, integrating anabolic, metabolic, and immunogenic complications in the cells. The systemic status of overfeeding, hyperlipidemia, and insulin resistance may contribute to the cardiac adjustment developed during weight gain. After losing weight, the heart's phenotype can be ostensibly restored to normal. However, some abnormalities still occur at the morphological (fibrosis) and proteomic levels.

Abbreviations

ACSL-1: long-chain-fatty-acid--CoA ligase 1; AMPK: AMP-activated protein kinase apolipoprotein A4 (APOA4); APOC3: apolipoprotein C3; CR: calorie restriction; DAVID: the database for annotation, visualization and integrated discovery; ECM: extracellular matrix; GLUT-1: solute carrier family 2, facilitated glucose transporter member 1; GLUT-4: solute carrier family 2, facilitated glucose transporter member 4; HDL: high-density lipoproteins; LDL: low-density lipoprotein; LV: left ventricle of the heart; mTOR; mammalian target of rapamycin; RBP4: retinol-binding protein 4; TTR: transthyretin.

Declarations

research, analyzed data and wrote the manuscript; MP performed research; JLK provided administrative support and corrected the paper. All authors approved final version of manuscript.

References

1. Roth J, Qiang X, Marbán SL, Redelt H, Lowell BC. The obesity pandemic: where have we been and where are we going? Obes Res [Internet]. United States; 2004;12 Suppl 2:88S-101S. Available from: https://pubmed.ncbi.nlm.nih.gov/15601956

2. (NCD-RisC) NCDRFC. Worldwide trends in body-mass index, underweight, overweight, and obesity from 1975 to 2016: a pooled analysis of 2416 population-based measurement studies in 128·9 million children, adolescents, and adults. Lancet (London, England) [Internet]. 2017/10/10. Elsevier; 2017;390:2627–42. Available from: https://pubmed.ncbi.nlm.nih.gov/29029897

3. Skinner AC, Ravanbakht SN, Skelton JA, Perrin EM, Armstrong SC. Prevalence of Obesity and Severe Obesity in US Children, 1999-2016. Pediatrics [Internet]. 2018;141:e20173459. Available from: https://pubmed.ncbi.nlm.nih.gov/29483202

4. Bray GA, Heisel WE, Afshin A, Jensen MD, Dietz WH, Long M, et al. The Science of Obesity Management: An Endocrine Society Scientific Statement. Endocr Rev [Internet]. Endocrine Society; 2018;39:79–132. Available from: https://pubmed.ncbi.nlm.nih.gov/29518206

5. Pi-Sunyer X. The medical risks of obesity. Postgrad Med [Internet]. 2009;121:21–33. Available from: https://pubmed.ncbi.nlm.nih.gov/19940414

6. Oparil S, Acelajado MC, Bakris GL, Berlowitz DR, Cífková R, Dominiczak AF, et al. Hypertension. Nat Rev Dis Prim [Internet]. 2018;4:18014. Available from: https://pubmed.ncbi.nlm.nih.gov/29565029

7. Cavalera M, Wang J, Frangogiannis NG. Obesity, metabolic dysfunction, and cardiac fibrosis: pathophysiological pathways, molecular mechanisms, and therapeutic opportunities. Transl Res [Internet]. 2014/05/10. 2014;164:323–35. Available from: https://pubmed.ncbi.nlm.nih.gov/24880146

8. Frangogiannis NG. The Extracellular Matrix in Ischemic and Nonischemic Heart Failure. Circ Res [Internet]. 2019/06/20. 2019;125:117–46. Available from: https://pubmed.ncbi.nlm.nih.gov/31219741

9. Cuspidi C, Rescaldani M, Sala C, Grassi G. Left-ventricular hypertrophy and obesity: a systematic review and meta-analysis of echocardiographic studies. J Hypertens [Internet]. England; 2014;32:16–25. Available from: https://pubmed.ncbi.nlm.nih.gov/24309485

10. Jia G, Aroor AR, Martinez-Lemus LA, Sowers JR. Overnutrition, mTOR signaling, and cardiovascular diseases. Am J Physiol Regul Integr Comp Physiol [Internet]. 2014/09/24. American Physiological Society; 2014;307:R1198–206. Available from: https://pubmed.ncbi.nlm.nih.gov/25253086

11. Xu L, Brink M. mTOR, cardiomyocytes and inflammation in cardiac hypertrophy. Biochim Biophys Acta [Internet]. 2016/01/08. Netherlands; 2016;1863:1894–903. Available from: https://pubmed.ncbi.nlm.nih.gov/26775585

12. Furtado MB, Nim HT, Boyd SE, Rosenthal NA. View from the heart: cardiac fibroblasts in development, scarring and regeneration. Development [Internet]. England; 2016;143:387–97. Available from: https://pubmed.ncbi.nlm.nih.gov/26839342

13. Ranjan P, Kumari R, Verma SK. Cardiac Fibroblasts and Cardiac Fibrosis: Precise Role of Exosomes. Front cell Dev Biol [Internet]. Frontiers Media S.A.; 2019;7:318. Available from: https://pubmed.ncbi.nlm.nih.gov/31867328

14. Alpert MA, Omran J, Mehra A, Ardhanari S. Impact of obesity and weight loss on cardiac performance and morphology in adults. Prog Cardiovasc Dis [Internet]. 2013/10/26. United States; 2014;56:391–400. Available from: https://pubmed.ncbi.nlm.nih.gov/24438730

15. McDowell K, Petrie MC, Raihan NA, Logue J. Effects of intentional weight loss in patients with obesity and heart failure: a systematic review. Obes Rev [Internet]. 2018/07/27. England; 2018;19:1189–204. Available from: https://pubmed.ncbi.nlm.nih.gov/30051959

16. Finer N. Weight loss for patients with obesity and heart failure. Eur Heart J [Internet]. England; 2019;40:2139–41. Available from: https://pubmed.ncbi.nlm.nih.gov/31180494

17. Mahajan R, Stokes M, Elliott A, Munawar DA, Khokhar KB, Thiyagarajah A, et al. Complex interaction of obesity, intentional weight loss and heart failure: a systematic review and meta-analysis. Heart [Internet]. 2019/09/17. England; 2020;106:58–68. Available from: https://pubmed.ncbi.nlm.nih.gov/31530572

18. Rai AJ, Gelfand CA, Haywood BC, Warunek DJ, Yi J, Schuchard MD, et al. HUPO Plasma Proteome Project specimen collection and handling: towards the standardization of parameters for plasma proteome samples. Proteomics [Internet]. Germany; 2005;5:3262–77. Available from: https://pubmed.ncbi.nlm.nih.gov/16052621

19. Chen J, Lee SK, Abd-Elgaliel WR, Liang L, Galende E-Y, Hajjar RJ, et al. Assessment of cardiovascular fibrosis using novel fluorescent probes. PLoS One [Internet]. Public Library of Science; 2011;6:e19097–e19097. Available from: https://pubmed.ncbi.nlm.nih.gov/21533060

20. Schindelin J, Arganda-Carreras I, Frise E, Kaynig V, Longair M, Pietzsch T, et al. Fiji: an open-source platform for biological-image analysis. Nat Methods [Internet]. 2012;9:676–82. Available from: https://pubmed.ncbi.nlm.nih.gov/22743772

21. Huang DW, Sherman BT, Lempicki RA. Bioinformatics enrichment tools: paths toward the comprehensive functional analysis of large gene lists. Nucleic Acids Res [Internet]. 2008/11/25. Oxford University Press; 2009;37:1–13. Available from: https://pubmed.ncbi.nlm.nih.gov/19033363

22. Huang DW, Sherman BT, Lempicki RA. Systematic and integrative analysis of large gene lists using DAVID bioinformatics resources. Nat Protoc [Internet]. England; 2009;4:44–57. Available from: https://pubmed.ncbi.nlm.nih.gov/19131956

23. Quispe R, Elshazly MB, Zhao D, Toth PP, Puri R, Virani SS, et al. Total cholesterol/HDL-cholesterol ratio discordance with LDL-cholesterol and non-HDL-cholesterol and incidence of atherosclerotic cardiovascular disease in primary prevention: The ARIC study. Eur J Prev Cardiol [Internet].

2019;2047487319862401–2047487319862401. Available from: https://pubmed.ncbi.nlm.nih.gov/31291776

24. Cheng SWY, Fryer LGD, Carling D, Shepherd PR. Thr2446 is a novel mammalian target of rapamycin (mTOR) phosphorylation site regulated by nutrient status. J Biol Chem [Internet]. 2004/02/17. United States; 2004;279:15719–22. Available from: https://pubmed.ncbi.nlm.nih.gov/14970221

25. Leguisamo NM, Lehnen AM, Machado UF, Okamoto MM, Markoski MM, Pinto GH, et al. GLUT4 content decreases along with insulin resistance and high levels of inflammatory markers in rats with metabolic syndrome. Cardiovasc Diabetol [Internet]. BioMed Central; 2012;11:100. Available from: https://pubmed.ncbi.nlm.nih.gov/22897936

26. Shao D, Tian R. Glucose Transporters in Cardiac Metabolism and Hypertrophy. Compr Physiol [Internet]. 2015;6:331–51. Available from: https://pubmed.ncbi.nlm.nih.gov/26756635

27. Ebeling P, Koistinen HA, Koivisto VA. Insulin-independent glucose transport regulates insulin sensitivity. FEBS Lett [Internet]. England; 1998;436:301–3. Available from: https://pubmed.ncbi.nlm.nih.gov/9801136

28. Li LO, Grevengoed TJ, Paul DS, Ilkayeva O, Koves TR, Pascual F, et al. Compartmentalized acyl-CoA metabolism in skeletal muscle regulates systemic glucose homeostasis. Diabetes [Internet]. 2014/07/28. American Diabetes Association; 2015;64:23–35. Available from: https://pubmed.ncbi.nlm.nih.gov/25071025

29. Schisler JC, Grevengoed TJ, Pascual F, Cooper DE, Ellis JM, Paul DS, et al. Cardiac energy dependence on glucose increases metabolites related to glutathione and activates metabolic genes controlled by mechanistic target of rapamycin. J Am Heart Assoc [Internet]. Blackwell Publishing Ltd; 2015;4:e001136. Available from: https://pubmed.ncbi.nlm.nih.gov/25713290

30. Yu D, Tomasiewicz JL, Yang SE, Miller BR, Wakai MH, Sherman DS, et al. Calorie-Restriction-Induced Insulin Sensitivity Is Mediated by Adipose mTORC2 and Not Required for Lifespan Extension. Cell Rep [Internet]. 2019;29:236-248.e3. Available from: https://pubmed.ncbi.nlm.nih.gov/31577953

31. Ingenbleek Y. The Retinol Circulating Complex Releases Hormonal Ligands During Acute Stress Disorders. Front Endocrinol (Lausanne) [Internet]. Frontiers Media S.A.; 2018;9:487. Available from: https://pubmed.ncbi.nlm.nih.gov/30233492

32. Sharma M, Khan S, Rahman S, Singh LR. The Extracellular Protein, Transthyretin Is an Oxidative Stress Biomarker. Front Physiol [Internet]. Frontiers Media S.A.; 2019;10:5. Available from: https://pubmed.ncbi.nlm.nih.gov/30733681

33. Ingenbleek Y, Bernstein LH. Plasma Transthyretin as a Biomarker of Lean Body Mass and Catabolic States. Adv Nutr [Internet]. American Society for Nutrition; 2015;6:572–80. Available from: https://pubmed.ncbi.nlm.nih.gov/26374179

34. Yang Q, Graham TE, Mody N, Preitner F, Peroni OD, Zabolotny JM, et al. Serum retinol binding protein 4 contributes to insulin resistance in obesity and type 2 diabetes. Nature [Internet]. England; 2005;436:356–62. Available from: https://pubmed.ncbi.nlm.nih.gov/16034410

35. Frey SK, Spranger J, Henze A, Pfeiffer AFH, Schweigert FJ, Raila J. Factors that influence retinol-binding protein 4-transthyretin interaction are not altered in overweight subjects and overweight subjects with type 2 diabetes mellitus. Metabolism [Internet]. 2009/06/18. United States; 2009;58:1386–92. Available from: https://pubmed.ncbi.nlm.nih.gov/19501859

36. Alpert MA. Obesity cardiomyopathy: pathophysiology and evolution of the clinical syndrome. Am J Med Sci [Internet]. United States; 2001;321:225–36. Available from: https://pubmed.ncbi.nlm.nih.gov/11307864

37. Sciarretta S, Volpe M, Sadoshima J. Mammalian target of rapamycin signaling in cardiac physiology and disease. Circ Res [Internet]. 2014;114:549–64. Available from: https://pubmed.ncbi.nlm.nih.gov/24481845

38. Ormazabal V, Nair S, Elfeky O, Aguayo C, Salomon C, Zuñiga FA. Association between insulin resistance and the development of cardiovascular disease. Cardiovasc Diabetol [Internet]. BioMed Central; 2018;17:122. Available from: https://pubmed.ncbi.nlm.nih.gov/30170598

39. Grevengoed TJ, Martin SA, Katunga L, Cooper DE, Anderson EJ, Murphy RC, et al. Acyl-CoA synthetase 1 deficiency alters cardiolipin species and impairs mitochondrial function. J Lipid Res [Internet]. 2015/07/01. The American Society for Biochemistry and Molecular Biology; 2015;56:1572–82. Available from: https://pubmed.ncbi.nlm.nih.gov/26136511

40. Coleman RA, Lewin TM, Van Horn CG, Gonzalez-Baró MR. Do long-chain acyl-CoA synthetases regulate fatty acid entry into synthetic versus degradative pathways? J Nutr [Internet]. United States; 2002;132:2123–6. Available from: https://pubmed.ncbi.nlm.nih.gov/12163649

41. Herrero P, Peterson LR, McGill JB, Matthew S, Lesniak D, Dence C, et al. Increased myocardial fatty acid metabolism in patients with type 1 diabetes mellitus. J Am Coll Cardiol [Internet]. 2006/01/18. United States; 2006;47:598–604. Available from: https://pubmed.ncbi.nlm.nih.gov/16458143

42. Bertero E, Maack C. Metabolic remodelling in heart failure. Nat Rev Cardiol [Internet]. England; 2018;15:457–70. Available from: https://pubmed.ncbi.nlm.nih.gov/29915254

43. Nagoshi T, Yoshimura M, Rosano GMC, Lopaschuk GD, Mochizuki S. Optimization of cardiac metabolism in heart failure. Curr Pharm Des [Internet]. Bentham Science Publishers; 2011;17:3846–53. Available from: https://pubmed.ncbi.nlm.nih.gov/21933140

44. Vileigas DF, Harman VM, Freire PP, Marciano CLC, Sant'Ana PG, de Souza SLB, et al. Landscape of heart proteome changes in a diet-induced obesity model. Sci Rep [Internet]. Nature Publishing Group UK; 2019;9:18050. Available from: https://pubmed.ncbi.nlm.nih.gov/31792287

45. Behring JB, Kumar V, Whelan SA, Chauhan P, Siwik DA, Costello CE, et al. Does reversible cysteine oxidation link the Western diet to cardiac dysfunction? FASEB J Off Publ Fed Am Soc Exp Biol. 2014;28:1975–87.

46. Andres AM, Kooren JA, Parker SJ, Tucker KC, Ravindran N, Ito BR, et al. Discordant signaling and autophagy response to fasting in hearts of obese mice: Implications for ischemia tolerance. Am J Physiol Heart Circ Physiol. 2016;311:H219-28.

47. Sverdlov AL, Elezaby A, Behring JB, Bachschmid MM, Luptak I, Tu VH, et al. High fat, high sucrose diet causes cardiac mitochondrial dysfunction due in part to oxidative post-translational modification of mitochondrial complex II. J Mol Cell Cardiol. 2015;78:165–73.

48. Rindler PM, Plafker SM, Szweda LI, Kinter M. High dietary fat selectively increases catalase expression within cardiac mitochondria. J Biol Chem. 2013;288:1979–90.

49. Romanick SS, Ulrich C, Schlauch K, Hostler A, Payne J, Woolsey R, et al. Obesity-mediated regulation of cardiac protein acetylation: parallel analysis of total and acetylated proteins via TMT-tagged mass spectrometry. Biosci Rep. 2018;38.

50. Xu M-Y, Ye Z-S, Song X-T, Huang R-C. Differences in the cargos and functions of exosomes derived from six cardiac cell types: a systematic review. Stem Cell Res Ther [Internet]. BioMed Central; 2019;10:194. Available from: https://pubmed.ncbi.nlm.nih.gov/31248454

51. Yu H, Wang Z. Cardiomyocyte-Derived Exosomes: Biological Functions and Potential Therapeutic Implications. Front Physiol [Internet]. Frontiers Media S.A.; 2019;10:1049. Available from: https://pubmed.ncbi.nlm.nih.gov/31481897

52. Wang X, Gu H, Huang W, Peng J, Li Y, Yang L, et al. Hsp20-Mediated Activation of Exosome Biogenesis in Cardiomyocytes Improves Cardiac Function and Angiogenesis in Diabetic Mice. Diabetes [Internet]. 2016/06/09. American Diabetes Association; 2016;65:3111–28. Available from: https://pubmed.ncbi.nlm.nih.gov/27284111

53. Qu B, Jia Y, Liu Y, Wang H, Ren G, Wang H. The detection and role of heat shock protein 70 in various nondisease conditions and disease conditions: a literature review. Cell Stress Chaperones [Internet]. 2015/07/03. Springer Netherlands; 2015;20:885–92. Available from: https://pubmed.ncbi.nlm.nih.gov/26139132

54. Di Naso FC, Porto RR, Fillmann HS, Maggioni L, Padoin AV, Ramos RJ, et al. Obesity depresses the anti-inflammatory HSP70 pathway, contributing to NAFLD progression. Obesity (Silver Spring) [Internet]. 2014/10/08. United States; 2015;23:120–9. Available from: https://pubmed.ncbi.nlm.nih.gov/25292174

55. Kobori H, Urushihara M, Xu JH, Berenson GS, Navar LG. Urinary angiotensinogen is correlated with blood pressure in men (Bogalusa Heart Study). J Hypertens [Internet]. 2010;28:1422–8. Available from: https://pubmed.ncbi.nlm.nih.gov/20375906

56. Kurdi M, Booz GW. New take on the role of angiotensin II in cardiac hypertrophy and fibrosis. Hypertens (Dallas, Tex 1979) [Internet]. 2011/04/18. 2011;57:1034–8. Available from: https://pubmed.ncbi.nlm.nih.gov/21502563

57. Kanter JE, Shao B, Kramer F, Barnhart S, Shimizu-Albergine M, Vaisar T, et al. Increased apolipoprotein C3 drives cardiovascular risk in type 1 diabetes. J Clin Invest [Internet]. American Society for Clinical Investigation; 2019;130:4165–79. Available from: https://pubmed.ncbi.nlm.nih.gov/31295146

58. Taskinen M-R, Borén J. Why Is Apolipoprotein CIII Emerging as a Novel Therapeutic Target to Reduce the Burden of Cardiovascular Disease? Curr Atheroscler Rep [Internet]. Springer US; 2016;18:59.

Available from: https://pubmed.ncbi.nlm.nih.gov/27613744

59. Uhlén M, Fagerberg L, Hallström BM, Lindskog C, Oksvold P, Mardinoglu A, et al. Proteomics. Tissue-based map of the human proteome. Science [Internet]. United States; 2015;347:1260419. Available from: https://pubmed.ncbi.nlm.nih.gov/25613900

60. Thul PJ, Åkesson L, Wiking M, Mahdessian D, Geladaki A, Ait Blal H, et al. A subcellular map of the human proteome. Science [Internet]. 2017/05/11. United States; 2017;356:eaal3321. Available from: https://pubmed.ncbi.nlm.nih.gov/28495876

61. Uhlen M, Zhang C, Lee S, Sjöstedt E, Fagerberg L, Bidkhori G, et al. A pathology atlas of the human cancer transcriptome. Science [Internet]. United States; 2017;357:eaan2507. Available from: https://pubmed.ncbi.nlm.nih.gov/28818916

62. Khatri N, Sagar A, Peddada N, Choudhary V, Chopra BS, Garg V, et al. Plasma gelsolin levels decrease in diabetic state and increase upon treatment with F-actin depolymerizing versions of gelsolin. J Diabetes Res [Internet]. 2014/11/12. Hindawi Publishing Corporation; 2014;2014:152075. Available from: https://pubmed.ncbi.nlm.nih.gov/25478578

63. Cheng Y, Hu X, Liu C, Chen M, Wang J, Wang M, et al. Gelsolin Inhibits the Inflammatory Process Induced by LPS. Cell Physiol Biochem [Internet]. 2017/01/20. Germany; 2017;41:205–12. Available from: https://pubmed.ncbi.nlm.nih.gov/28135711

64. Kelsh R, You R, Horzempa C, Zheng M, McKeown-Longo PJ. Regulation of the innate immune response by fibronectin: synergism between the III-1 and EDA domains. PLoS One [Internet]. Public Library of Science; 2014;9:e102974–e102974. Available from: https://pubmed.ncbi.nlm.nih.gov/25051083

65. Wang Y, Kinzie E, Berger FG, Lim SK, Baumann H. Haptoglobin, an inflammation-inducible plasma protein. Redox Rep [Internet]. England; 2001;6:379–85. Available from: https://pubmed.ncbi.nlm.nih.gov/11865981

66. Fries E, Kaczmarczyk A. Inter-alpha-inhibitor, hyaluronan and inflammation. Acta Biochim Pol [Internet]. Poland; 2003;50:735–42. Available from: https://pubmed.ncbi.nlm.nih.gov/14515153

67. Joe B, Nagaraju A, Gowda LR, Basrur V, Lokesh BR. Mass-spectrometric identification of T-kininogen I/thiostatin as an acute-phase inflammatory protein suppressed by curcumin and capsaicin. PLoS One [Internet]. Public Library of Science; 2014;9:e107565–e107565. Available from: https://pubmed.ncbi.nlm.nih.gov/25299597

68. Jonigk D, Al-Omari M, Maegel L, Müller M, Izykowski N, Hong J, et al. Anti-inflammatory and immunomodulatory properties of α1-antitrypsin without inhibition of elastase. Proc Natl Acad Sci U S A [Internet]. 2013/08/23. National Academy of Sciences; 2013;110:15007–12. Available from: https://pubmed.ncbi.nlm.nih.gov/23975926

69. Ritchie RF, Palomaki GE, Neveux LM, Navolotskaia O, Ledue TB, Craig WY. Reference distributions for the negative acute-phase serum proteins, albumin, transferrin and transthyretin: a practical, simple and clinically relevant approach in a large cohort. J Clin Lab Anal [Internet]. John Wiley & Sons, Inc.; 1999;13:273–9. Available from: https://pubmed.ncbi.nlm.nih.gov/10633294

70. Janeway CA Jr, Travers P WM. Immunobiology: The Immune System in Health and Disease. [Internet]. 5th edition. New York: Garland Science; 2001. Available from: https://www.ncbi.nlm.nih.gov/books/NBK27100/

71. Bonnans C, Chou J, Werb Z. Remodelling the extracellular matrix in development and disease. Nat Rev Mol Cell Biol [Internet]. 2014;15:786–801. Available from: https://pubmed.ncbi.nlm.nih.gov/25415508

72. Sheng Y, Lv S, Huang M, Lv Y, Yu J, Liu J, et al. Opposing effects on cardiac function by calorie restriction in different-aged mice. Aging Cell [Internet]. 2017/08/11. John Wiley and Sons Inc.; 2017;16:1155–67. Available from: https://pubmed.ncbi.nlm.nih.gov/28799249

73. Aquila-Pastir LA, DiPaola NR, Matteo RG, Smedira NG, McCarthy PM, Moravec CS. Quantitation and distribution of beta-tubulin in human cardiac myocytes. J Mol Cell Cardiol [Internet]. England; 2002;34:1513–23. Available from: https://pubmed.ncbi.nlm.nih.gov/12431450

74. Engebretsen KVT, Lunde IG, Strand ME, Waehre A, Sjaastad I, Marstein HS, et al. Lumican is increased in experimental and clinical heart failure, and its production by cardiac fibroblasts is induced by mechanical and proinflammatory stimuli. FEBS J [Internet]. 2013/04/02. England; 2013;280:2382–98. Available from: https://pubmed.ncbi.nlm.nih.gov/23480731

75. Krishnan A, Li X, Kao W-Y, Viker K, Butters K, Masuoka H, et al. Lumican, an extracellular matrix proteoglycan, is a novel requisite for hepatic fibrosis. Lab Invest [Internet]. 2012/09/24. 2012;92:1712–25. Available from: https://pubmed.ncbi.nlm.nih.gov/23007134

76. Pilling D, Vakil V, Cox N, Gomer RH. TNF-α-stimulated fibroblasts secrete lumican to promote fibrocyte differentiation. Proc Natl Acad Sci U S A [Internet]. 2015/09/08. National Academy of Sciences; 2015;112:11929–34. Available from: https://pubmed.ncbi.nlm.nih.gov/26351669

77. Mohammadzadeh N, Lunde IG, Andenæs K, Strand ME, Aronsen JM, Skrbic B, et al. The extracellular matrix proteoglycan lumican improves survival and counteracts cardiac dilatation and failure in mice subjected to pressure overload. Sci Rep [Internet]. Nature Publishing Group UK; 2019;9:9206. Available from: https://pubmed.ncbi.nlm.nih.gov/31235849

78. Theocharis AD, Manou D, Karamanos NK. The extracellular matrix as a multitasking player in disease. FEBS J [Internet]. 2019/04/11. England; 2019;286:2830–69. Available from: https://pubmed.ncbi.nlm.nih.gov/30908868

79. Christensen G, Herum KM, Lunde IG. Sweet, yet underappreciated: Proteoglycans and extracellular matrix remodeling in heart disease. Matrix Biol [Internet]. 2018/01/12. Netherlands; 2019;75–76:286–99. Available from: https://pubmed.ncbi.nlm.nih.gov/29337052

80. Wang X, Lu Y, Xie Y, Shen J, Xiang M. Emerging roles of proteoglycans in cardiac remodeling. Int J Cardiol [Internet]. 2018/11/28. Netherlands; 2019;278:192–8. Available from: https://pubmed.ncbi.nlm.nih.gov/30528626

81. Sengupta P. The Laboratory Rat: Relating Its Age With Human's. Int J Prev Med [Internet]. Medknow Publications & Media Pvt Ltd; 2013;4:624–30. Available from: https://pubmed.ncbi.nlm.nih.gov/23930179

82. Kuo AA, Inkelas M, Slusser WM, Maidenberg M, Halfon N. Introduction of solid food to young infants. Matern Child Health J [Internet]. Springer US; 2011;15:1185–94. Available from: https://pubmed.ncbi.nlm.nih.gov/20842523

83. Larqué E, Labayen I, Flodmark C-E, Lissau I, Czernin S, Moreno LA, et al. From conception to infancy - early risk factors for childhood obesity. Nat Rev Endocrinol [Internet]. 2019/07/03. England; 2019;15:456–78. Available from: https://pubmed.ncbi.nlm.nih.gov/31270440

84. Newens KJ, Walton J. A review of sugar consumption from nationally representative dietary surveys across the world. J Hum Nutr Diet [Internet]. 2015/10/10. John Wiley and Sons Inc.; 2016;29:225–40. Available from: https://pubmed.ncbi.nlm.nih.gov/26453428

85. Redman LM, Ravussin E. Caloric restriction in humans: impact on physiological, psychological, and behavioral outcomes. Antioxid Redox Signal [Internet]. 2010/08/28. Mary Ann Liebert, Inc.; 2011;14:275–87. Available from: https://pubmed.ncbi.nlm.nih.gov/20518700

86. Conti CR. Obesity and Weight Loss. Eur Cardiol [Internet]. Radcliffe Cardiology; 2018;13:93–4. Available from: https://pubmed.ncbi.nlm.nih.gov/30697351
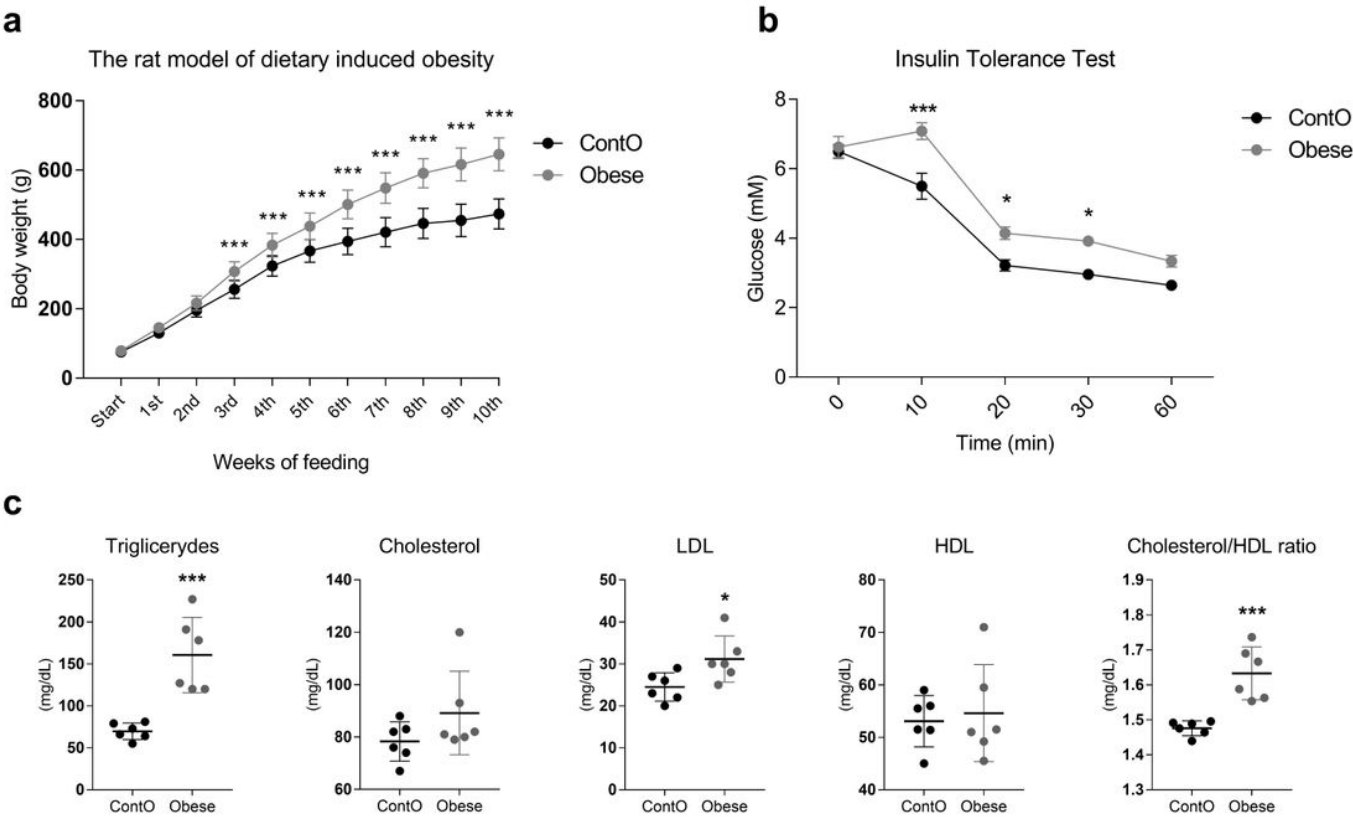
Figures

Fig.1

Figure 1

Characteristics of the obesity phenotype in rats fed with a human-mimicking Western diet for 10 weeks. As a consequence of high-calorie feeding, the animals gained weight intensively (a) and developed insulin resistance (b) with hyperlipidemia and hypercholesterolemia (c). Two-way ANOVA with Sidak's multiple comparison test (a, b) and the Student's T-test or Mann-Whitney test were used for analyzing the data (*p<0.5, **p<0.01, ***p<0.001).
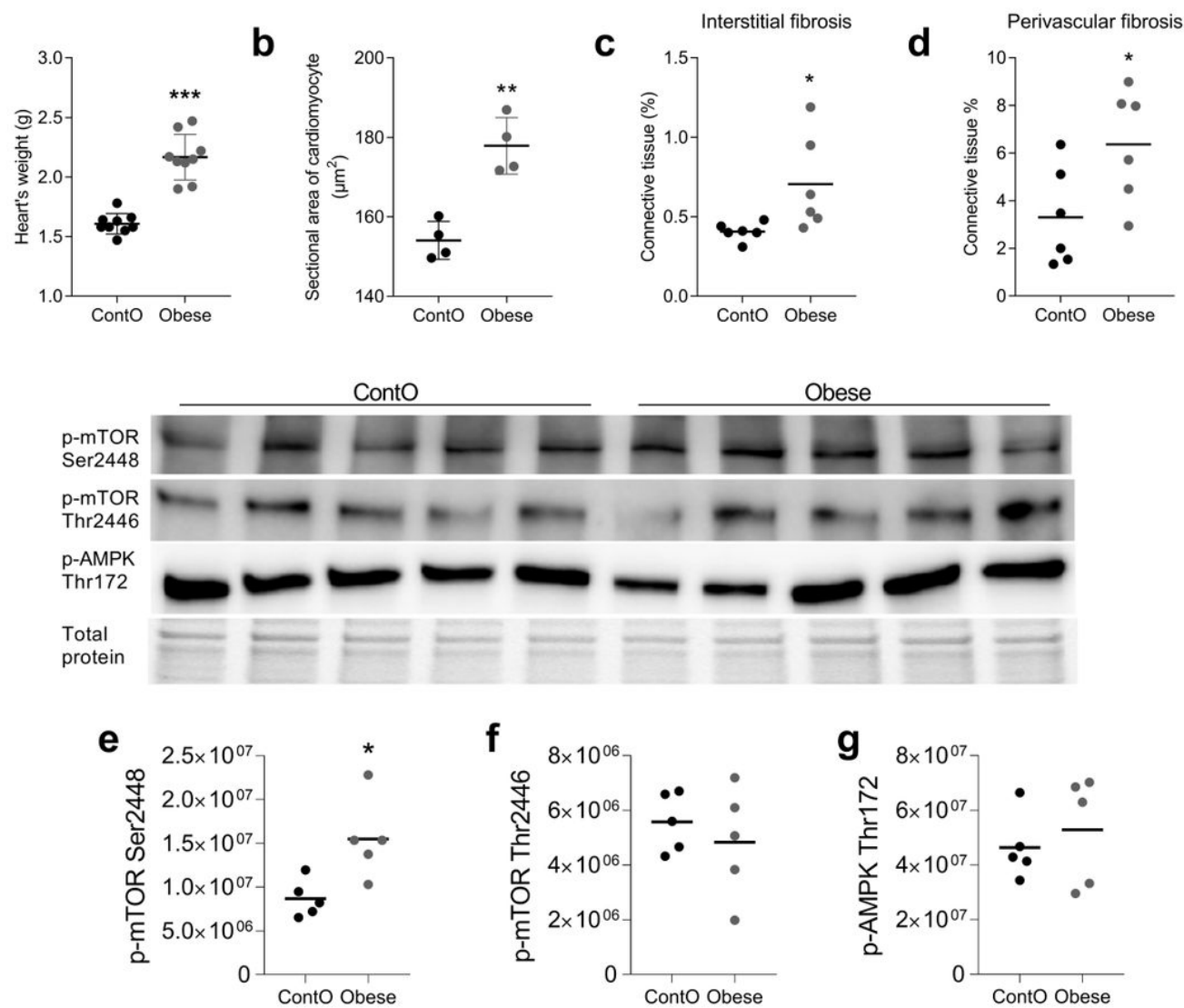

Fig.2

Figure 2

Hallmarks of obesity cardiomyopathy in rats. The hearts of obese animals were heavier (a) with enlarged myocytes (b). The oversized hearts contained higher levels of fibrotic tissue both in the non-vessel (c) and vessel containing (d) areas. The expression of phospho-mTOR on ser2448 (e) but not on Thr2446 (f) was higher in the LV of obese rats, suggesting the up-regulation of this anabolic pathway. No significant differences were observed with regard to of AMPK activity (g). The Student's T-test or Mann-Whitney test were used for analyzing the data (*p<0.5, **p<0.01, ***p<0.001).
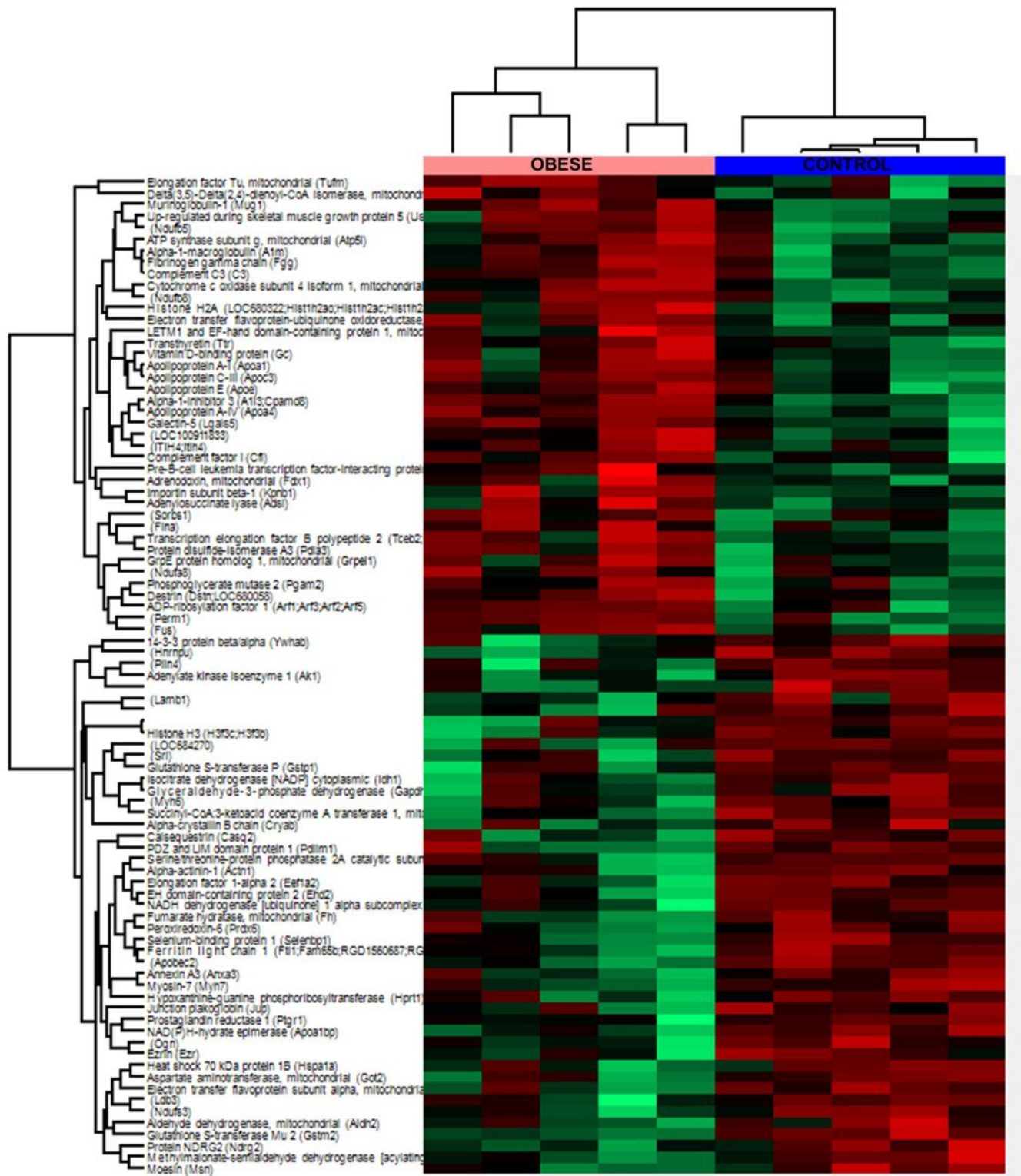
Figure 3

Global proteomic profile of the cardiac muscle of obese rats. The amount of 87 proteins differed in the LV tissue of obese rats as compared to homogenous samples from control individuals.
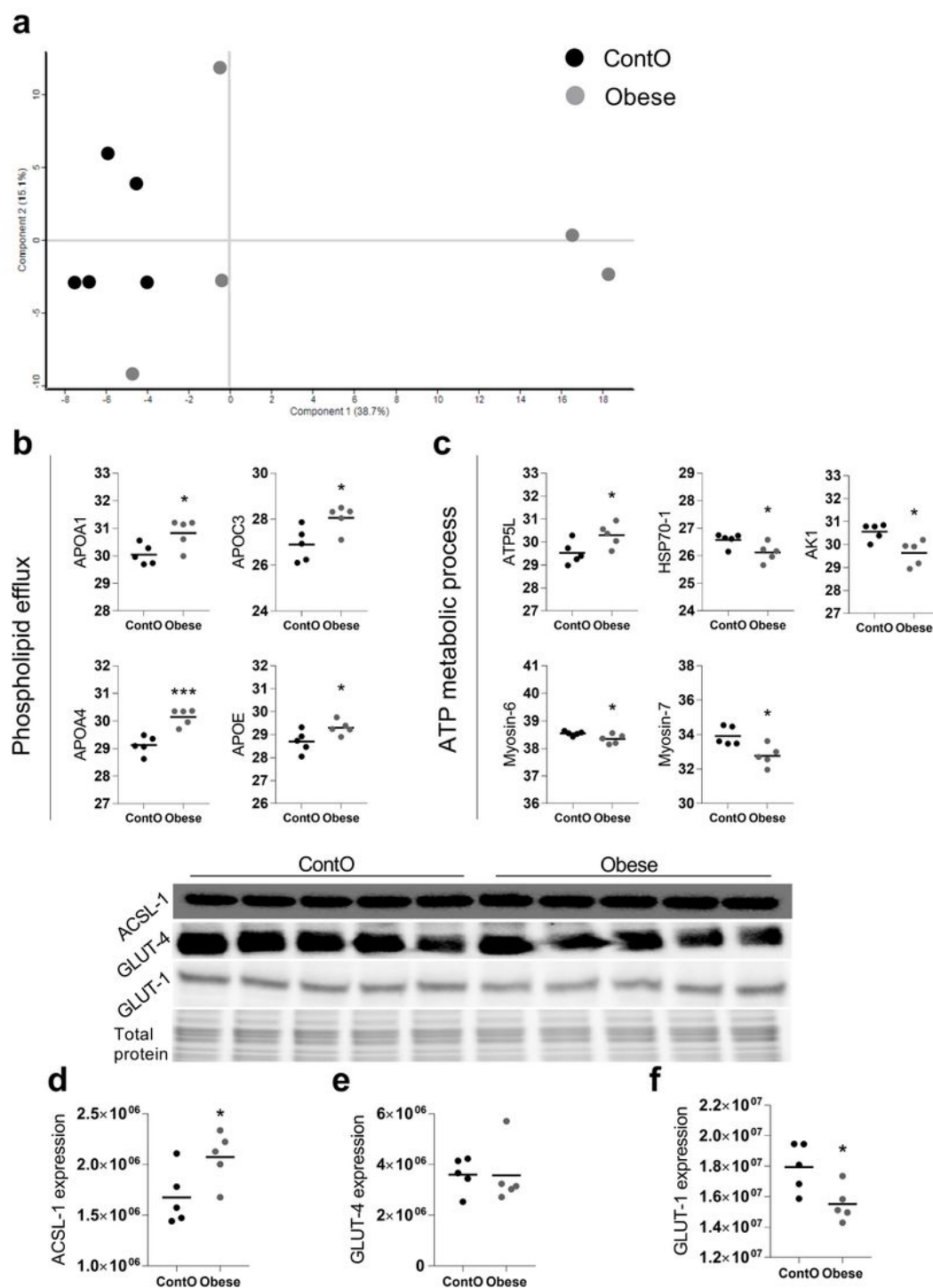
Fig. 4

Figure 4

Molecular processes changed in the heart muscle of obese rats. A scaling plot of individual proteomes revealed the relatively homogenous composition in the control group (contO) and the more dispersed proteomic phenotype in experimental (obese) animals (a).Two biological processes: (b) the directed movement of a phospholipid out of a cell or organelle (p=0.024), and (c) the chemical reactions and pathways involving ATP (p=0.043), were significantly changed in the tissue (Bonferoni correction). By

using the INTACT database we determined that the pool of all significantly changed proteins interacted with GLUT-4 (27 proteins, $p<0.001$, Fisher correction) and ACSL-1 (4 proteins, $p=0.0035$, Fisher correction), suggesting that these proteins may be impacted by obesity. The evaluation of the protein expression by means of WB showed that the cardiac expression of ACSL-1 (d, $p=0.045$) but not GLUT-4 (e) was changed (increased) in obese rats. GLUT-1 is the next glucose carrier in cardiomyocytes beyond GLUT-4, and its expression was downregulated in obese rats (f, $p=0.026$). The Student's T-test was used for analyzing the data (*$p<0.5$, ***$p<0.001$). ACSL-1: long-chain-fatty-acid-CoA ligase 1;AK1: adenylate kinase isoenzyme 1; ATP5L: ATP synthase subunit; GLUT-1: solute carrier family 2, facilitated glucose transporter member 1; GLUT-4: solute carrier family 2, facilitated glucose transporter member 4; HSP70-1: heat shock 70 kDa protein 1A.
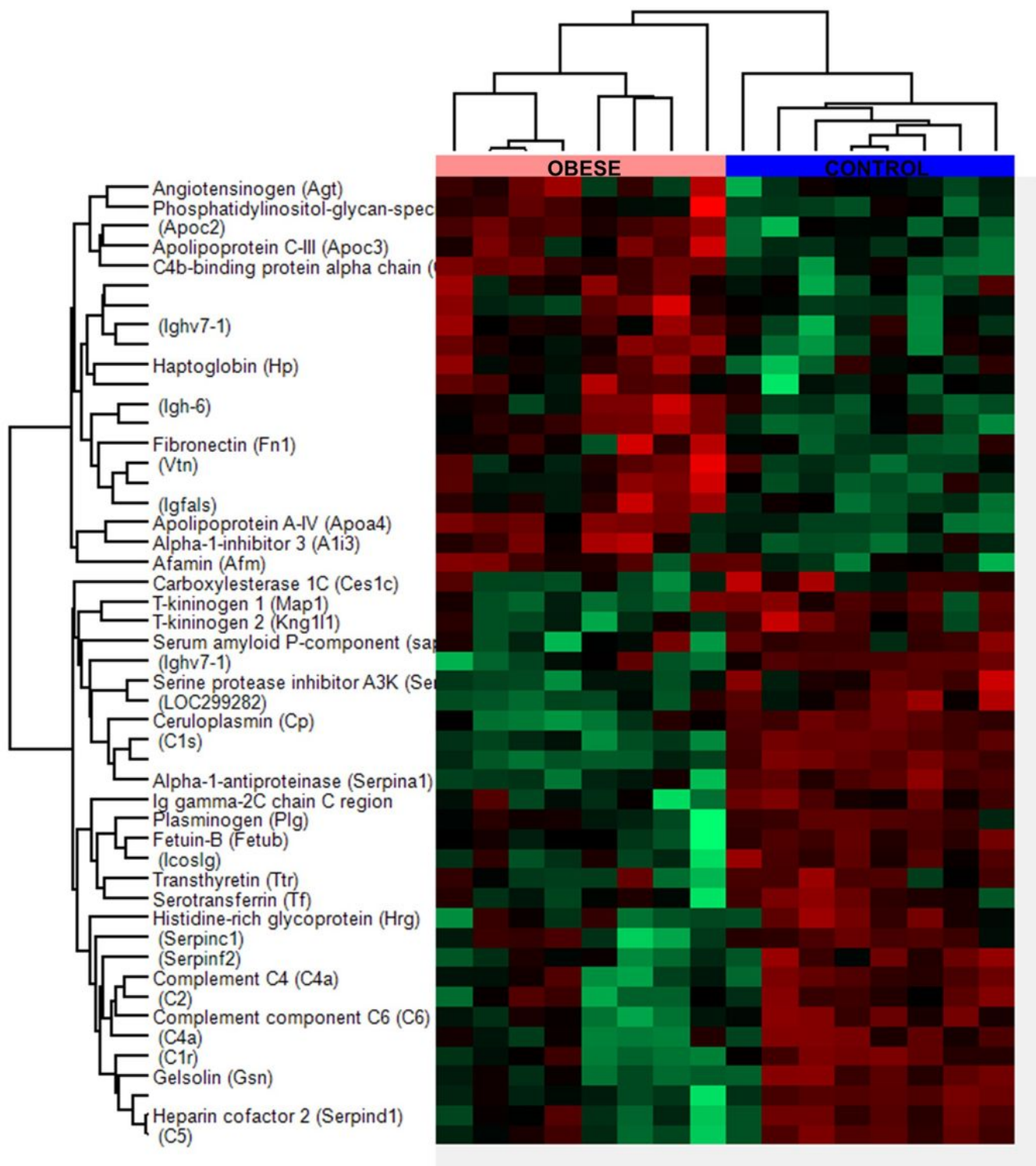
Figure 5

Global proteomic profile of plasma of obese rats. The amount of 49 proteins differed in the plasma of obese rats as compared to homogenous samples from control individuals.
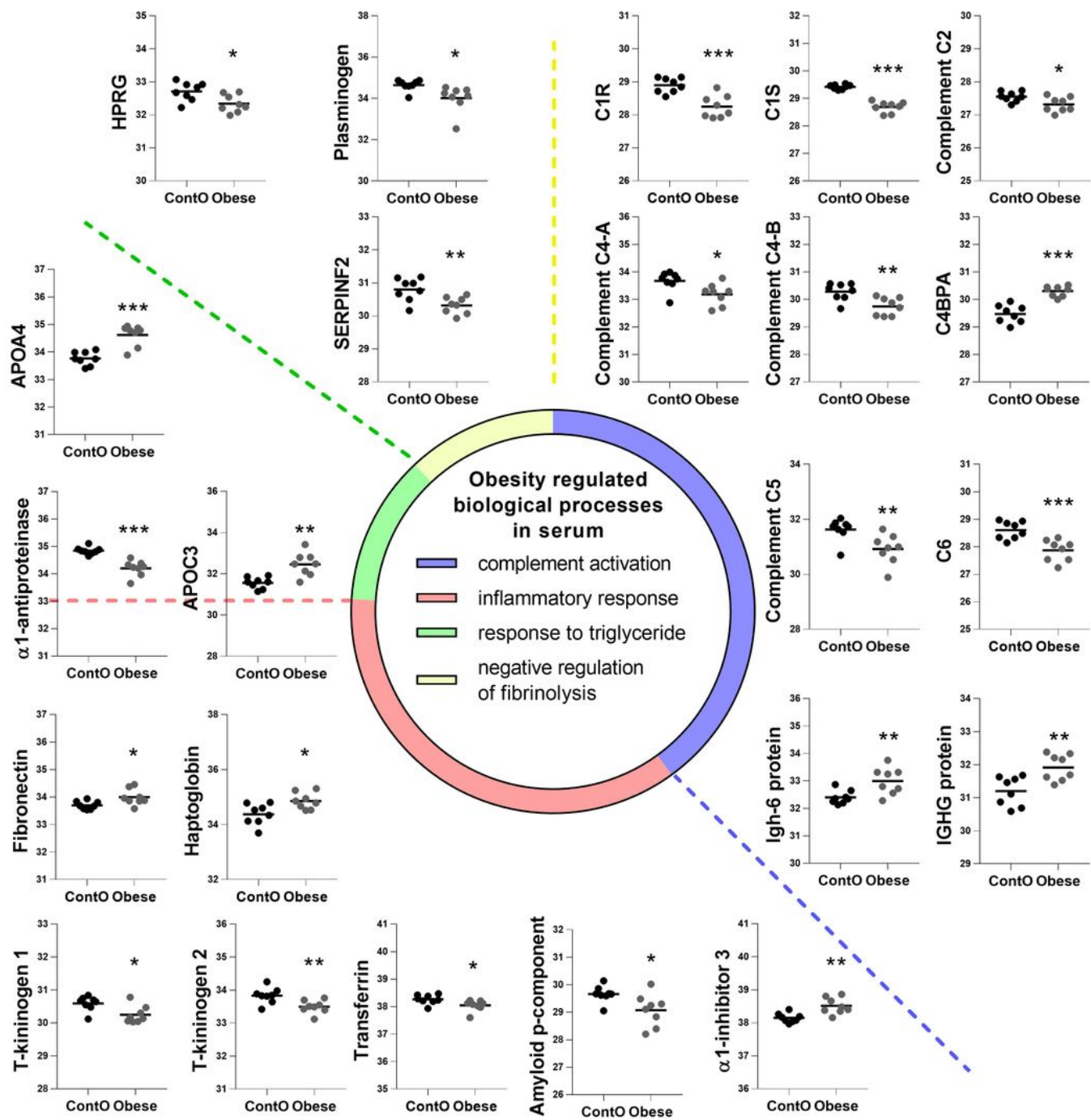
Fig.6

Figure 6

Clustering of the plasma proteins significantly changed in obese rats. Based on the GO:BP (DAVID functional annotation results with Bonferroni statistics) database, plasma proteins were assigned to their respective particular biological function. Most of the proteins (36%) were involved in the negative regulation of endopeptidase activity (p<0.001, not shown; refer to Supplemental Data for details). 17% of the proteins were involved in immunological regulation (GO:0006956~complement activation,

GO:0006958~complement activation). In addition, 17% of molecules participated in the pro-inflammatory response (GO:0006953~acute-phase response, $p<0.001$; GO:0045087~innate immune response, $p<0.01$; GO:0006954~inflammatory response, $p<0.05$). The next biological process changed in the plasma of obese rats included the abnormal level of proteins involved in the regulation of any process that results in a systemic change as a result of a triglyceride stimulus (GO:0034014~response to triglyceride, $p<0.05$). The pool of proteins (3 molecules) involved in processes that stop, prevent, or reduce the frequency, rate, or extent of fibrinolysis resulting in the removal of small blood clots was downregulated in the plasma of obese animals (GO:0051918~negative regulation of fibrinolysis, $p<0.05$). The Student's T-test was used for analyzing the data (*$p<0.5$, **$p<0.01$, ***$p<0.001$). APOA4: apolipoprotein A-IV; APOC3: apolipoprotein C-III; C1R: complement C1r subcomponent; C1S: complement C1s subcomponent; C4BPA: C4b-binding protein alpha chain; C6: complement component C6; HPRG: histidine-rich glycoprotein; SERPINF2: serpin family F member 2.
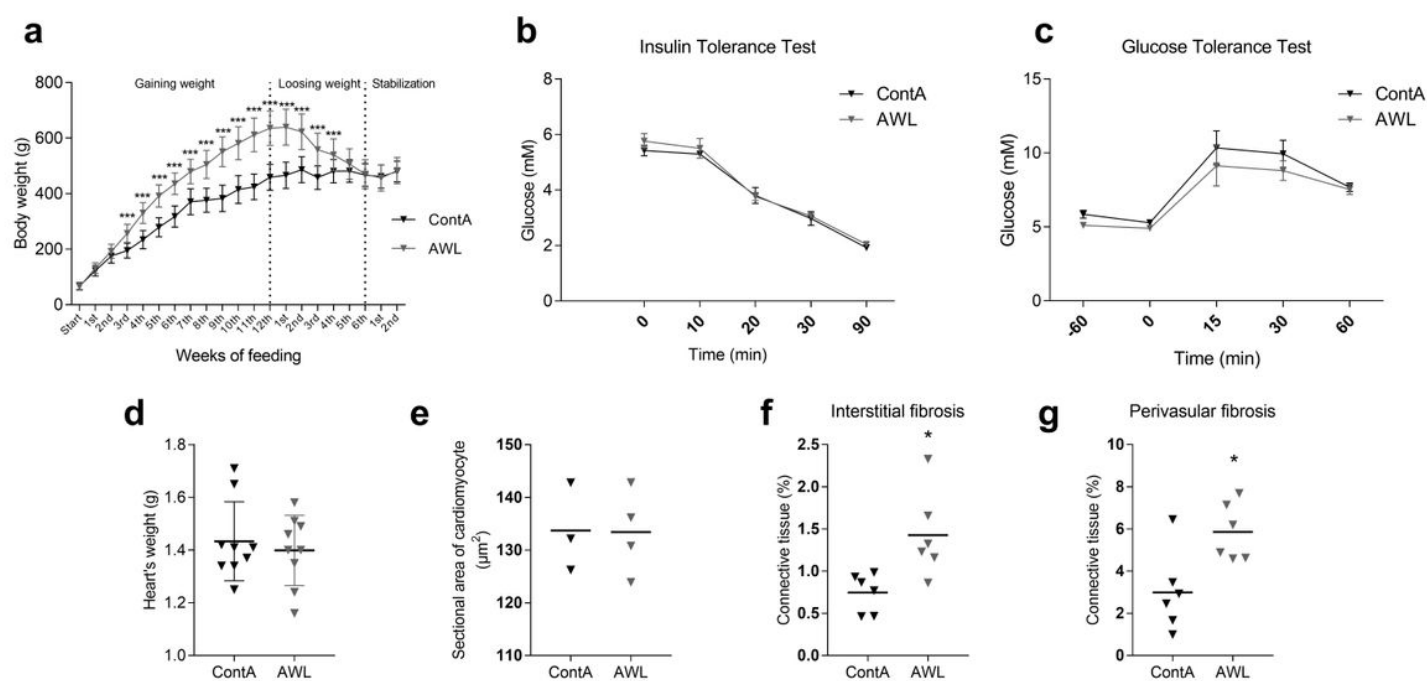

Figure 7

Characteristics of rats after weight loss. After 12 weeks of feeding with a human-mimicking Western diet, rats intensively gained weight (a), developing the obesity phenotype. Obese animals were subjected to CR for 6 weeks to lose weight. For the next two weeks, animals from the experimental (After Weight Loss, AWL) and control (ContA) groups received an isocaloric amount of calories (stabilization period) to ensure stable body weight. After weight loos, the rats did not show features of insulin resistance (b, c). The mass of cardiac muscle (d) and size of the cardiomyocytes (e) were restored after weight loss in rats which were previously obese. However, the interstitial (f) and perivascular (g) amount of connective tissue

was elevated in these animals. Two-way ANOVA with Sidak's multiple comparison test (a, b, c) and the Student's T-test or Mann-Whitney test were used for analyzing the data (*p<0.5, ***p<0.001).

Supplementary Files

This is a list of supplementary files associated with this preprint. Click to download.

- Supplementaldata.xlsx
- Supplementaldata.xlsx